


ESI-MS quantitation of increased sphingomyelin in Niemann-Pick disease type B HDL

Ching Yin Lee,* Alain Lesimple,[†] Åsmund Larsen,[§] Orval Mamer,[†] and Jacques Genest^{1,*}

Cardiovascular Genetics Laboratory,* Department of Medicine, and Mass Spectrometry Unit,[†] McGill University, Montréal, Canada; and Department of Chemistry,[§] University of Oslo, Oslo, Norway

Abstract HDLs have been proposed to have antiatherogenic properties because of their role in reverse cholesterol transport as lipid acceptors. To elucidate the phospholipid profile of these particles, we used electrospray ionization mass spectrometry to examine the phosphatidylcholine (PC) and sphingomyelin (SM) composition of HDLs purified from plasma and nascently generated *in vitro* from fibroblasts. We also quantitatively compared the phospholipids present in these lipoproteins between normal and Niemann-Pick disease type B (NPD-B) subjects characterized by sphingomyelinase (SMase) deficiency. We demonstrated that plasma HDLs from NPD-B were significantly enriched in SM by an average of 28%, particularly the palmitoyl SM (with an increase of 95%), which accounted for ~25–44% of total SM molecular species. Similarly, we observed an increase of ~63% in total SM levels in nascent HDLs prepared from NPD-B fibroblasts. Although PC levels in nascent HDLs were comparable between control and NPD-B cells, there was a 95% increase in total PC levels similar to that of SM in plasma HDLs extracted from NPD-B subjects.  These data provide insight into the structure of HDLs and identify potential new roles for SMase in lipoprotein metabolism.—Lee, C. Y., A. Lesimple, Å. Larsen, O. Mamer, and J. Genest. **ESI-MS quantitation of increased sphingomyelin in Niemann-Pick disease type B HDL.** *J. Lipid Res.* 2005. 46: 1213–1228.

Supplementary key words electrospray ionization-mass spectrometry • phospholipids • sphingomyelin phosphodiesterase-1 gene • sphingomyelinase • high density lipoprotein

Niemann-Pick disease type B (NPD-B) is an autosomal recessive disorder caused by mutations in the sphingomyelin phosphodiesterase 1 (SMPD-1) gene, which codes for the acid sphingomyelinase (SMase). Deficiency of SMase leads to the accumulation of sphingomyelin (SM) and cholesterol in many organs, notably liver and spleen (1). Lipid accumulation is also observed in cells by various methods (2). We previously reported an association of SMPD-1 and reduced HDL-cholesterol (HDL-C) (3). HDL is important in lipid metabolism, and low HDL-C levels are correlated

with a greater incidence of atherosclerosis. HDL particles are formed through a stepwise maturation process: lipid-free apolipoprotein A-I (apoA-I) is initially lipidated with phospholipids to form disc-like pre β HDLs. These nascent particles then become substrates for the accumulation of cholesterol and phospholipids effluxed from cells. LCAT promotes the esterification of their cholesterol content, forming spherical HDL particles with an inner core of cholesteryl esters. These α -migrating particles absorb more lipids and finally mature into HDL₂ particles (4, 5).

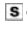
Recent work has underscored the importance of lipid composition for the conformation and stability of HDL particles (6, 7). The study of phospholipids, notably phosphatidylcholine (PC) and SM, is primarily important because they are the main building blocks for all cellular membranes and because they perform a diverse number of other functions, such as signaling or as a component of lipid rafts (8, 9). Recently, the role of SM in HDLs has been the subject of investigation because of its characteristic high gel-to-liquid crystalline phase transition temperature (10). Bolin and Jonas (11) and Rye, Hime, and Barter (12) independently observed that increasing the SM content in reconstituted apoA-I-containing particles was associated with significant reductions in the rate of cholesterol esterification by LCAT, which is essential for HDL maturation. Thus, we hypothesized that the lack of SMase in NPD-B subjects affects the phospholipid profile of their HDL particles, which could in turn lead to rapid catabolism and reduced HDL-C levels in plasma.

At present, mass spectrometry is the most sophisticated technique for assessing the phospholipid content of biological samples because of its high sensitivity and unmatched specificity, as it directly analyzes phospholipids as intact

Abbreviations: apoA-I, apolipoprotein A-I; CID, collision-induced decomposition; ESI-MS, electrospray ionization-mass spectrometry; HDL-C, high density lipoprotein-cholesterol; NPD-B, Niemann-Pick disease type B; PC, phosphatidylcholine; SM, sphingomyelin; SMase, sphingomyelinase; SMPD-1, sphingomyelin phosphodiesterase-1.

¹ To whom correspondence should be addressed.

e-mail: jacques.genest@muhc.mcgill.ca

 The online version of this article (available at <http://www.jlr.org>) contains an additional figure and two tables.

Manuscript received 11 January 2005 and in revised form 15 February 2005.

Published, JLR Papers in Press, March 1, 2005.

DOI 10.1194/jlr.M500011-JLR200

molecules and preserves the information contained in their chemical structures. For example, collision-induced decomposition (CID) of PC and SM in positive ion mode leads to the formation of an ion at m/z 184 characteristic of their polar head group, the phosphocholine. In negative ion mode, CID of PC identifies the fatty acyl substituents esterified to the glycerophospholipid backbone (13–15). Here, we used electrospray ionization-mass spectrometry (ESI-MS) and internal standard addition to qualitatively and quantitatively analyze and compare the PC and SM contents of total HDL isolated from plasma and nascent HDL particles generated from fibroblasts of normal and NPD-B subjects. We report increased SM in the lipid moiety of HDLs from NPD-B as another pathophysiological hallmark of this sphingolipid disorder.

MATERIALS AND METHODS

Materials

All phospholipid standards were purchased from Avanti Polar Lipids (Birmingham, AL) except N20:0 SM, which was from Matreya LLC (Pleasant Gap, PA). All solvents were HPLC-grade and were purchased from Fisher Scientific (Pittsburgh, PA). All chemical reagents were of analytical grade and were purchased from Sigma-Aldrich (St. Louis, MO). AccuBond amino solid-phase extraction columns were from Agilent Technologies (Palo Alto, CA). Amicon Ultra 15 concentrators were from Millipore (Bedford, MA). All tissue culture reagents were from Gibco Invitrogen (Burlington, Ontario, Canada).

Study subjects

Controls and patients were selected from the Preventive Cardiology/Lipid Clinic of the McGill University Health Centre in Montreal, Canada. The research protocol was reviewed and approved by the institutional Ethics Committee. Signed informed consent was obtained for blood sampling, DNA analysis, and fibroblast cultures. Four normolipidemic subjects were selected as controls. We examined two siblings (subject 303, a 49 year-old man, and his sister, subject 301, a 47 year old woman) from a family affected with NPD-B. Both of them were compound heterozygous for $\Delta R608$ and $R441X$ at the SMPD-1 gene, as described previously (3). Both underwent coronary artery bypass graft procedures for severe coronary artery disease in their 40s. Skin fibroblast cultures were established as described previously (16).

HDL preparation

Total HDL fractions ($1.091 < d < 1.210$) were isolated from plasma by ultracentrifugation in a potassium bromide gradient (17). Their apoA-I concentrations and cholesterol contents were measured by standard ELISA and enzymatic assay. HDL was also generated by loading for 24 h 20 $\mu\text{g}/\text{ml}$ purified apoA-I (Academy Bio-Medical Co., Houston, TX) onto 150 mm fibroblast cells that had been incubated previously for 1 day with 20 $\mu\text{g}/\text{ml}$ LDL. Medium was collected and concentrated with Amicon Ultra 15 filters with a cutoff molecular weight of 10,000. The cellular protein concentration was measured by the Lowry method and used to normalize lipid quantitation. All HDL samples were stored at -80°C until extraction.

Lipid extraction

Before extraction, samples were mixed with known amounts of internal standards (C19:0/C19:0 PC and N17:0 SM) that have been shown to be absent in the samples. The lipids were ex-

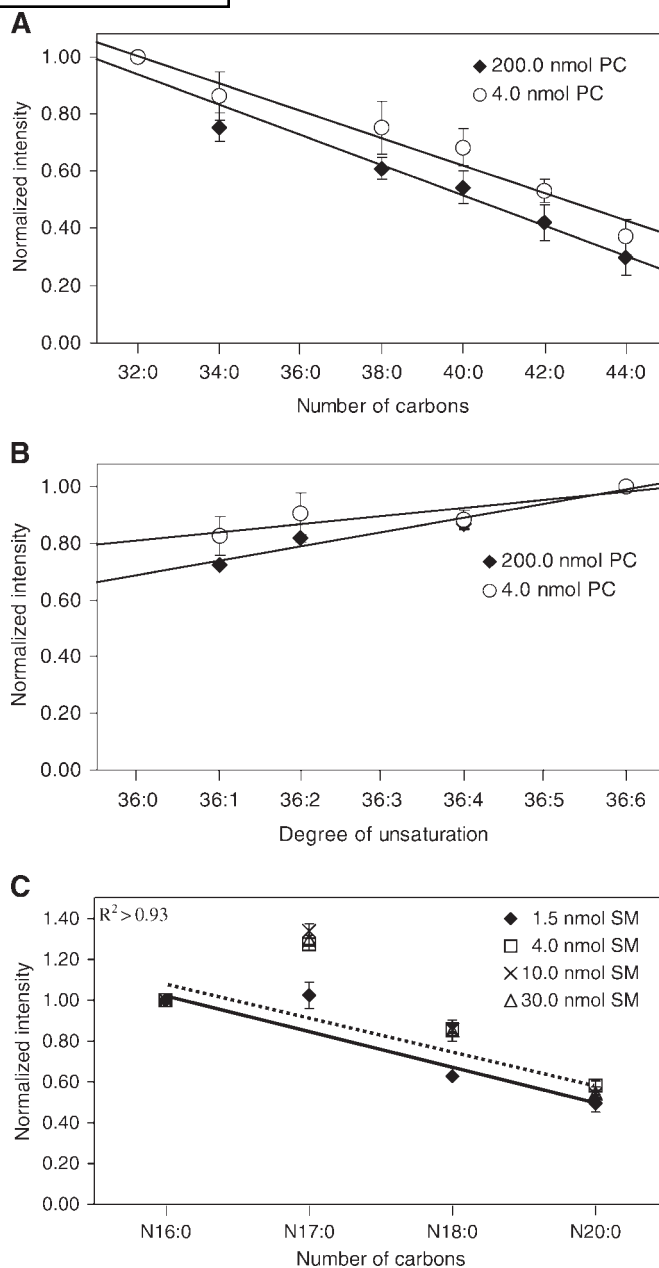


Fig. 1. A: Effects of acyl chain length on instrument responses for phosphatidylcholine (PC). Equimolar amounts of C16:0/C16:0 PC (32:0), C16:0/C18:0 PC (34:0), C19:0/C19:0 PC (38:0), C20:0/C20:0 PC (40:0), C21:0/C21:0 PC (42:0), and C22:0/C22:0 PC (44:0) were mixed and extracted as described in Materials and Methods. The data represent means \pm SD of three different preparations. B: Effects of the degree of unsaturation on instrument responses for PC. Equimolar amounts of C18:0/C18:1 PC (36:1), C18:1/C18:1 PC (36:2), C18:2/C18:2 PC (36:4), and C18:3/C18:3 PC (36:6) were mixed and extracted as described in Materials and Methods. The data represent means \pm SD of three different preparations. C: Effects of acyl chain length on instrument responses for sphingomyelin (SM). Equimolar amounts of N16:0 SM, N17:0 SM, N18:0 SM, and N20:0 SM were mixed and extracted as described in Materials and Methods. The data represent means \pm SD of three different preparations.

TABLE 1. Correction factors (chain length effects) for PC quantitation

PC (200 nmol) Carbon No.	(Y) ^a Relative Ionization Effect	Correction Factor (vs. C19:0 Standard)	PC (4 nmol) Carbon No.	(Y) ^b Relative Ionization Effect	Correction Factor (vs. C19:0 Standard)
32:0	0.940	1.51	32:0	1.000	1.41
34:0	0.834	1.34	34:0	0.904	1.27
36:0	0.727	1.17	36:0	0.808	1.14
38:0	0.621	1.00	38:0	0.711	1.00
40:0	0.515	0.83	40:0	0.615	0.86
42:0	0.408	0.66	42:0	0.519	0.73
44:0	0.302	0.49	44:0	0.423	0.59

PC, phosphatidylcholine.

^aY = 0.940 - 0.0532(X - 32); X = total carbon number. R² = 0.96. P (slope) < 0.001.

^bY = 1.000 - 0.0481(X - 32); X = total carbon number. R² = 0.96. P (slope) < 0.001.

tracted with chloroform-methanol (2:1) with 0.01% (w/v) 2,6-di-*tert*-butyl-4-methylphenol added with sonication as described previously (18). The organic layer was recovered and evaporated to dryness. The dried lipid was resuspended in chloroform and analyzed by ESI-MS within the same day. For lipid characterization, extracted lipids were purified further with AccuBond amino solid-phase extraction columns as described previously (19) to remove anionic phospholipids (i.e., phosphatidylglycerol, phosphatidic acid, and phosphatidylinositol).

Electrospray mass spectrometry

ESI-MS analysis was carried out in positive and negative ion modes using a Micromass Quattro II triple quadrupole mass spectrometer equipped with an electrospray source. Cellular and plasma HDL samples, diluted 14- and 42-fold, respectively, in chloroform-methanol (1:2) containing 25 mM ammonium acetate were infused at a flow rate of 120 μl/h. Data were accumulated in multiple-channel analysis mode, and analyses were carried out using MassLynx version 3.5 software. Nitrogen was used as drying gas (400 l/h) and a nebulizing gas (20 l/h). The electrospray capillary was set at 2.5 kV. ESI-MS analyses were carried out at a cone voltage of 45 V, a scan rate of 300 Da/s with an interscan delay of 0.1 s, and with scan ranges of 650–950 Da in the positive ion mode and 190–370 Da in the negative ion mode. The resolving power was set to obtain unit resolution. For PC characterization, ESI-MS/MS was used with argon as collision gas at a pressure of 0.9 × 10⁻³ mbar, and the collision energy was set to 50 eV. The mass axis of MS1 and MS2 were calibrated previously with water clusters using water containing 0.05% trifluoroacetic acid. For PC and SM quantitation, ESI-MS was used instead of ESI-MS/MS because the latter technique results in differential fragmentation rates for individual molecular species containing different acyl constituents that are highly sensitive to the collisional activation energy used (20).

HPLC-mass spectrometry

In a collaborative study, our plasma samples were analyzed separately by HPLC-MS as described previously (18) using an HPLC apparatus from Hewlett-Packard coupled online to a Quattro II mass spectrometer from Micromass. The phospholipids were separated on a LiChrospher 100 Diol (5 μm), 250 × 2 mm column (Merck, Darmstadt, Germany). Chloroform was used as mobile phase A, and mobile phase B was methanol containing 0.1% (v/v) formic acid and 0.05% (v/v) triethylamine made pH 5.3 with ammonia. Separation of phospholipid classes was achieved with a gradient starting at 5% mobile phase B, increasing to 30% B in 11 min, increasing further to 80% B in 3 min, held at 80% B for 4 min, and then decreasing back to 5% B in 2 min. The total run time was 30 min; the flow rate was 0.3 ml/min at ambient temperature. Ion source parameters were optimized in the positive ion mode with respect to the quasimolecular ions of the phospholipids. The cone voltage was set to 40 V. The electrospray capillary was set to 3.0 kV, the source block temperature was 100°C, and the nitrogen gas temperature was 250°C. The drying gas and nebulizer gas were optimized to 350 and 20 l/h, respectively. The detection of PC and SM in the complex phospholipid extract was performed in precursor ion scans at *m/z* 184, and their quantitation was based on multiple reaction monitoring transitions at *m/z* 184.

Data analysis

By means of direct infusion ESI-MS, PC and SM species were discriminated on the basis of 1) their characteristic *m/z* value, 2) precursor ion scan of *m/z* 184, 3) fragmentation analysis in negative scan mode for PC by ESI-MS/MS, and 4) isotopic patterns. Quantitation of the analyte species was performed in ESI-MS by comparisons of individual ion peak intensities with the addition of internal standards in known amounts (i.e., C19:0/PC and N17:0 SM) followed by correction for natural abundance of heavy isotope substitution. Each spectrum was accumulated for

TABLE 2. Correction factors (degree of unsaturation effects) for PC quantitation

PC (200 nmol) Degree of Unsaturation	(Y) ^a Relative Ionization Effect	Correction Factor (vs. C18:0)	PC (4 nmol) Degree of Unsaturation	(Y) ^b Relative Ionization Effect	Correction Factor (vs. C18:0)
39:0	0.685	1.00	39:0	0.810	1.00
39:1	0.736	1.07	39:1	0.839	1.04
39:2	0.787	1.15	39:2	0.867	1.07
39:3	0.839	1.22	39:3	0.896	1.11
39:4	0.890	1.30	39:4	0.924	1.14
39:5	0.941	1.37	39:5	0.953	1.18
39:6	0.992	1.45	39:6	0.981	1.21

^aY = 0.685 + 0.0512X; X = degree of unsaturation. R² = 0.96. P (slope) = 0.021.

^bY = 0.810 + 0.0285X; X = degree of unsaturation. R² = 0.77. P (slope) = 0.122.

12 min in multiple-channel analysis, smoothed (Savitzky Golay 2×0.50), background subtracted (polynomial order of 2, 1% below curve), and centroided on the top 80% with ion intensity based on area. It has been demonstrated that different molecular species of polar lipids have different ionization efficiencies depending on the acyl chain length and degree of unsaturation (21–23). Accordingly, the variations in instrument response attributable to these differential ionization efficiencies were corrected for PC and SM expressed in true molar abundances by factors determined in the calibration curves, which were obtained with equimolar concentrations of standards.

Statistical analysis

All experiments were done in triplicate, and the results are expressed as means \pm SD. All other statistical analysis was performed with GraphPad Prism software (San Diego, CA).

RESULTS

Instrument responses versus acyl chain length and degree of unsaturation

ESI-MS offers an attractive method for the analysis of phospholipid composition because of its “soft” ionization, high sensitivity, and specificity. Yet, precautions were taken in this quantitative study because different molecular species are not detected with equal efficiency. We established a response factor based on a calibration curve that related the intensity of the observed quasimolecular ion species to their carbon numbers and degrees of unsaturation. We used commercially available synthetic PC standards, including C16:0/C16:0 PC (32:0), C16:0/C18:0 PC (34:0), C19:0/C19:0 PC (38:0), C20:0/C20:0 PC (40:0), C21:0/C21:0 PC (42:0), and C22:0/C22:0 PC (44:0), to study the chain length effect. We used C18:0/C18:1 PC (36:1), C18:1/C18:1 PC (36:2), C18:2/C18:2 PC (36:4), and C18:3/C18:3 PC (36:6) to estimate the effect of the degree of unsaturation. The amounts of PC standard used in the subsequent PC quantitation of plasma and cellular samples were 200.0 and 4.0 nmol in 200 μ l of chloroform, respectively. These were further diluted 42- and 14-fold, respectively, before injection, leading to the final approximate concentrations of 23.8 and 1.40 nmol/ml for plasma and cellular samples. As reported previously (21–23), the instrument response decreased markedly and in a nearly linear manner with increasing acyl chain length (Fig. 1A). This effect became slightly more important when the overall lipid concentration increased from 4.0 to 200.0 nmol in 200 μ l of chloro-

form, as observed by Koivusalo et al. (21). In addition, the instrument response was markedly dependent on the degree of acyl chain unsaturation (Fig. 1B). It has been proposed (21) that the unsaturated species are more surface-active and compete more effectively for desorption. Additionally, the double bonds could weaken the intermolecular interactions in the droplet surface layer, thus enhancing the expulsion of the ions into the gas phase. **Tables 1, 2** summarize the correction factors based on the calibration curves in Fig. 1A, B, which were used to correct the experimental ion abundances to the true molar abundances (**Table 3**). These correction factors were deduced from the regression equations derived from the calibration curves, whose R^2 value indicates that our model fits our data well. The P value of the slopes for Fig. 1B was compromised only by the lack of standards (missing points) within the calculated best-fit line. For the quantitative analysis of SM, we established a calibration curve using only N16:0 SM, N17:0 SM, N18:0 SM, and N20:0 SM because synthetic SM species bracketing the profile of natural SM are not available (22). The amounts of SM standard used in the subsequent SM quantitation of plasma and cellular samples were 30.0 and 1.5 nmol in 200 μ l of chloroform, respectively. These were further diluted 42- and 14-fold, respectively, before injection, leading to the final approximate concentrations of 3.6 and 0.5 nmol/ml for plasma and cellular samples. Although there was a linearity of the chain length effects for the standards with even numbers of carbons, we observed that the signal intensity of N17:0 SM was higher than equimolar amounts of N16:0 (1.02- and 1.30-fold for 1.5 and 30.0 nmol SM in 200 μ l of chloroform, respectively). This zigzag odd-even effect was consistent for all four concentrations tested (1.5, 4.0, 10.0, and 30.0 nmol in 200 μ l of chloroform) (Fig. 1C). Odd-even effects for various physical properties have been reported (24, 25), and we believe that the markedly higher signal of N17:0 SM was caused by the difference in polarizability, leading to a different efficiency in ionization (24, 25).

Although both Koivusalo et al. (21) and DeLong et al. (23) have shown that increasing dilutions could reduce the complications caused by the differential effects of acyl chain length, unsaturation, and lipid concentration on instrument responses, we were limited by the heterogeneity of our biological samples containing more than 40 PC species we have characterized in small quantities. The op-

TABLE 3. Correction of ion abundance with respect to the C19:0/19:0 PC standard for the most common PC species

Chains	Species	Correction (Plasma HDL)	Correction (HDL from Fibroblasts)
C32:0	C16:0/C16:0	$I_{\text{relative}} \times (1/1.51)$	$I_{\text{relative}} \times (1/1.41)$
C34:2	C16:0/C18:2	$I_{\text{relative}} \times (1/1.34) \times (1/1.15)$	$I_{\text{relative}} \times (1/1.27) \times (1/1.07)$
C34:1	C16:0/C18:1	$I_{\text{relative}} \times (1/1.34) \times (1/1.07)$	$I_{\text{relative}} \times (1/1.27) \times (1/1.04)$
C36:4	C16:0/C20:4 and C18:2/C18:2	$I_{\text{relative}} \times (1/1.17) \times (1/1.30)$	$I_{\text{relative}} \times (1/1.14) \times (1/1.14)$
C36:3	C18:1/C18:2 and C16:0/C20:3	$I_{\text{relative}} \times (1/1.17) \times (1/1.22)$	$I_{\text{relative}} \times (1/1.14) \times (1/1.11)$
C36:2	C18:0/C18:2 and C18:1/C18:1 and C16:0/C20:2	$I_{\text{relative}} \times (1/1.17) \times (1/1.15)$	$I_{\text{relative}} \times (1/1.14) \times (1/1.07)$
C36:1	C18:0/C18:1	$I_{\text{relative}} \times (1/1.17) \times (1/1.07)$	$I_{\text{relative}} \times (1/1.14) \times (1/1.04)$

I_{relative} represents the apparent ion abundance of the analyte assessed by relating the ratio of the peak height of the analyte to that of the corresponding internal standards of known concentration. The calculation for true ion abundance is based on the correction factors that were extrapolated from the calibration curves in Fig. 1A, B and summarized in Tables 1, 2.

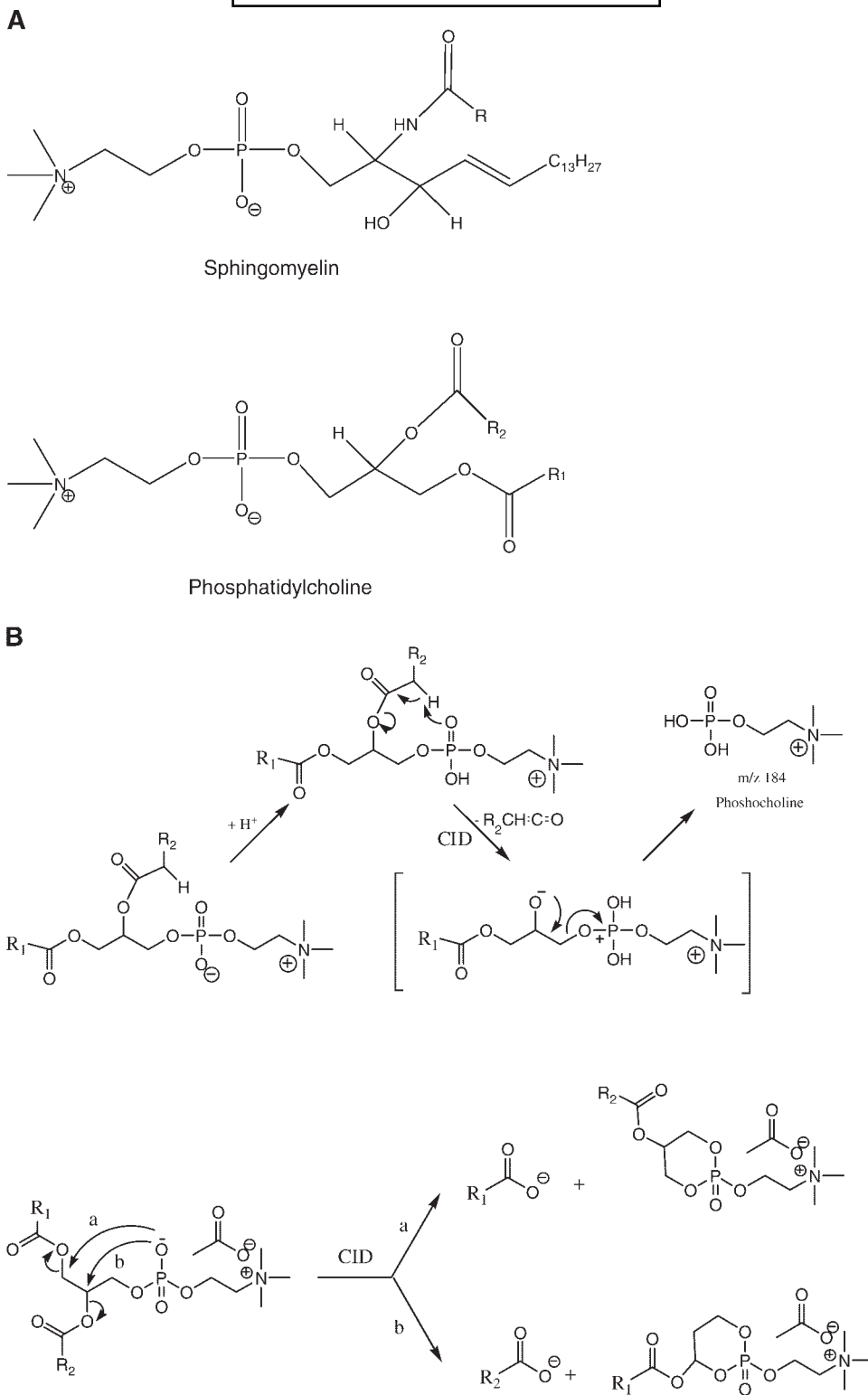


Fig. 2. A: Structures of SM and PC. Both SM and PC are choline-containing phospholipids that could be easily discriminated from other kinds of phospholipids because of their characteristic phosphocholine head group with m/z 184. The backbone of SM is formed by a long-chain amino alcohol, sphingosine, with a fatty acyl chain acylated at carbon 2 of the sphingosine moiety via an *N*-acyl ester linkage (ceramide). It has one nitrogen atom. In contrast, PC has no nitrogen in the backbone because it is formed by phosphatidic acid or 1,2-diacylglycerol with two fatty chains acylated via *O*-acyl ester linkages. B: Fragmentation mechanisms of PC in positive and negative ion modes. In positive ion mode, collision-induced decomposition (CID) of the positive protonated PC molecular ions ($[M+H]^+$) yields via a complex mechanism the expected phosphocholine ion at m/z 184. In negative ion mode, negatively charged PC acetate adduct ions $[M+CH_3COO]^-$ are dissociated into carboxylate anions via charge transfer, nucleophilic attack of the phosphate oxygen on the glycerol *sn*-1 and *sn*-2 carbons, and neutral loss of either a five- or six-membered ring of cyclolysophospholipid.

timial amounts of PC and SM standards (C19:0/C19:0 PC and N17:0 SM) we used were comparable with the amounts of the most dominant PC and SM species in the samples. As shown in Fig. 1A–C, we were not able to eliminate the effects of acyl chain length and degree of unsaturation on ion intensity under our experimental conditions, even when the concentrations were less than 1–2 nmol/ml. However, because their effects on the instrument responses were linear, we reasoned that we could adequately correct the quantitation by the factors extrapolated from the calibration curves (Tables 1–3). Although we could further dilute the samples and the standards until the effects of chain length and unsaturation diminished, as suggested by Koivusalo et al. (21), without affecting the analysis of the dominant PC species, the study of the other PC species as well as all SM species existing in much smaller quantities (up to <50-fold) would have been jeopardized by the decreased signal-to-noise ratio (a minimum of 3 was used in our study). Under our experimental conditions using the Micromass Quattro II triple quadrupole mass spectrometer, we determined that 42-fold dilution of the plasma samples and 14-fold dilution of the cellular samples enabled us to obtain the best resolution and sensitivity for PC and SM characterization and quantitation.

We also verified the effects of concentration on instrument responses, using 4.0, 25.0, 50.0, and 200.0 nmol of C19:0/C19:0 PC in 200 μ l of chloroform (diluted 42-fold before injection; data not shown) and 5.0, 15.0, and 30.0 nmol of N17:0 SM in 200 μ l of chloroform (diluted 42-fold before injection; data not shown). We have demonstrated that the PC and SM standards gave a dose-dependent linear response within the working concentration ranges we used in the phospholipid quantitation, thereby validating the linearity of our method.

Determination of SM and PC species based on their specific fragmentation mechanisms

The structures of PC and SM are shown in Fig. 2A. The main fragmentation pathway for these two choline-containing phospholipids in a triple quadrupole instrument has been described (26–28). In positive ion mode, CID of the protonated PC and SM molecular ions ($[M+H]^+$) gave the phosphocholine ion at m/z 184 derived from their phosphocholine head group. In addition, we used negative ion mode to characterize the acyl chains in PC species. The fragmentation pathway for PCs in negative ion mode has been proposed to occur via charge transfer, nucleophilic attack of the phosphate oxygen on the glycerol

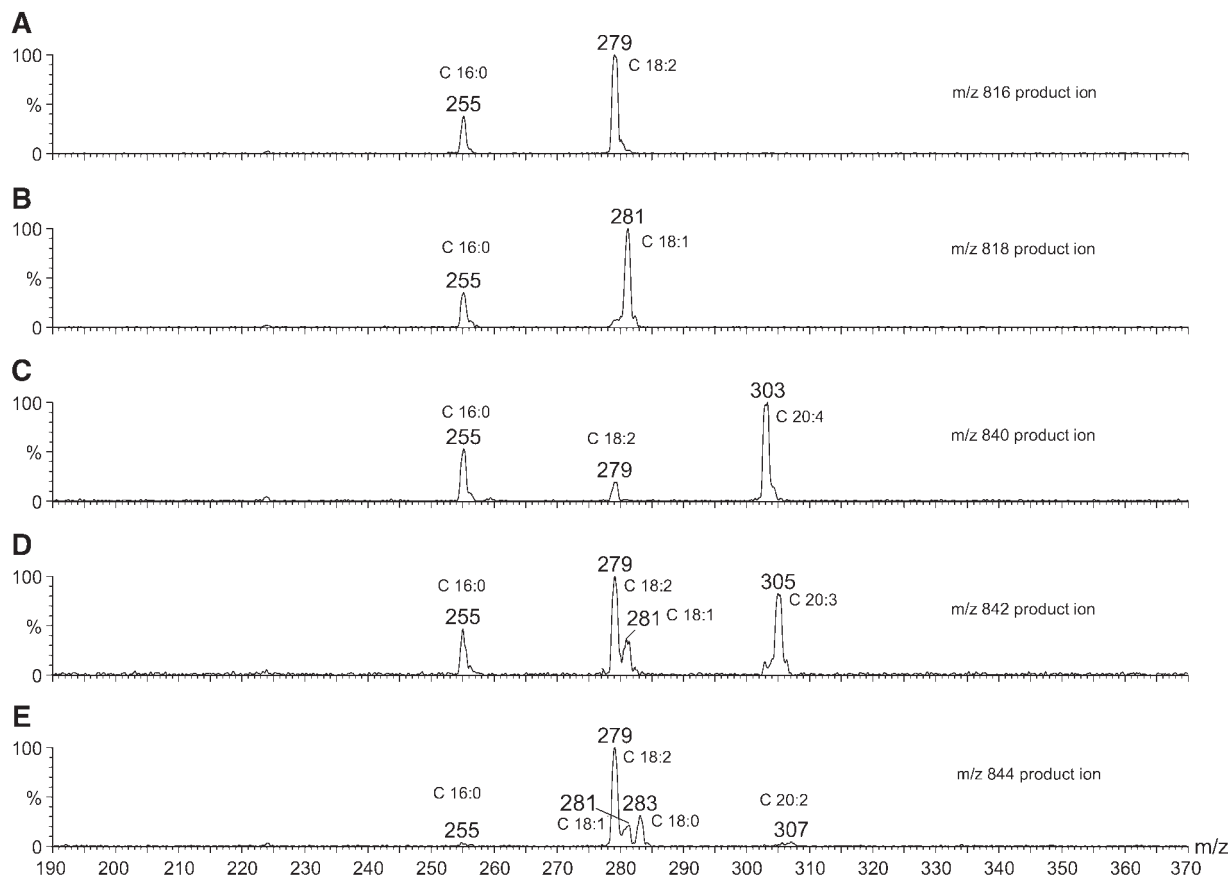


Fig. 3. Product ion spectra for acyl anions of nine major PC species in plasma HDL: linoleoyl-palmitoyl (C18:2/C16:0) PC at m/z 816 (A); oleoyl-palmitoyl (C18:1/C16:0) PC at m/z 818 (B); arachidonoyl-palmitoyl (C20:4/C16:0) and di-linoleoyl (C18:2/C18:2) PC at m/z 840 (C); linoleoyl-oleoyl (C18:2/C18:1) and eicosatrienoyl-palmitoyl (C20:3/C16:0) PC at m/z 842 (D); and linoleoyl-stearoyl (C18:2/C18:0) PC, di-oleoyl (C18:1/C18:1) PC, and eicosadienoyl-palmitoyl (C20:2/C16:0) PC at m/z 844 (E). The carboxylate ions were obtained in the negative ion mode (scan range 190–370 Da) by electrospray ionization-tandem mass spectrometry (ESI-MS/MS) as described in Materials and Methods.

erol *sn*-1 and *sn*-2 carbons, and formation of carboxylate anions with neutral loss of either a five- or six-membered ring of cyclolysophospholipid (26, 29) (Fig. 2B). Some productions gave evidence of several chain types, as shown in Fig. 3, which shows the product ion spectra of nine major PC species. A set of ESI-MS/MS scans for plasma HDLs and nascent HDLs from cells is available as supplementary data. During our PC characterization, we observed only very minor differences in chain composition and relative peak intensities between samples, as exemplified in the negative ion ESI-MS/MS of plasma HDL samples at *m/z* 842 in Fig. 4, even if the relative abundance of equivalent ions in the positive mode was different (Tables 4, 5). Therefore, we conclude that there was no significant difference between controls and patients for PC speciation.

It has been shown that no useful fragmentation can be obtained on SM compounds by negative ion ESI (18, 27). Although some authors have suggested the possibility of trace amounts of long-chain base groups other than d18:1 in SM (30), we have assumed for Tables 4, 5 that it was d18:1 and then determined the nature of the acyl chain from the pseudomolecular ion mass. Because of the possibilities of SM pseudomolecular ions hidden in the overlapping PC peak clusters, which could be discriminated only by isotopic correction in the direct infusion method, SM speciation was further confirmed by ESI-MS coupled online with HPLC, which allowed chromatographic separation of SM and PC before mass spectrometry. Figure 5 shows the HPLC-MS run of a plasma HDL sample and the major PC and SM species eluted at specific retention times. Figure 6 is an expansion of Fig. 5B, illustrating all SM species that we have identified.

Increased levels of SM in HDL extracted from NPD-B plasma

Although the HDL lipid content may vary slightly as a result of factors such as age, sex, race, diet, hormonal balance, physical exercise, etc. (31), we believe that it would be significantly affected in a diseased state, such as NPD-B, which is a sphingolipid disorder characterized by the accumulation of SM in many organs and cells (1, 2).

SM and PC molecular species in plasma HDL were identified as described in Materials and Methods and listed in Table 4 and Fig. 7. In total, we have characterized 13 SM species and 43 PC (acyl and ether) species: all SMs were almost exclusively saturated and monounsaturated with a relevant amount of long-chain fatty acid-containing species, most importantly N24:1 and N24:2 SM. The shortest SM species identified was 14 carbons long, but its concentration in the samples was very low. The most abundant ion was at *m/z* 703.7 (corresponding to N16:0 SM), which accounts for ~25–30% of total SM molecular species in control plasma HDL samples and more than 40% in NPD-B samples. Because the amount of PC was more than 9-fold greater than that of SM in plasma HDL analytes, PC ions, especially those of the dominant species, were easily identified. These were PCs with 34 and 36 carbons, including linoleoyl-palmitoyl (18:2/16:0) PC, linoleoyl-stearoyl (18:2/18:0) PC, di-oleoyl (18:1/18:1) PC, eicosadienoyl-palmitoyl (20:2/16:0) PC, arachidonoyl-palmitoyl (20:4/16:0) PC, di-linoleoyl (18:2/18:2) PC, oleoyl-palmitoyl (18:1/16:0) PC, linoleoyl-oleoyl (18:2/18:1) PC, and eicosatrienoyl-palmitoyl (20:3/16:0) PC. The minor species included PCs with asymmetric fatty acids of 14 to 24 carbons long with up to six double bonds. All SM

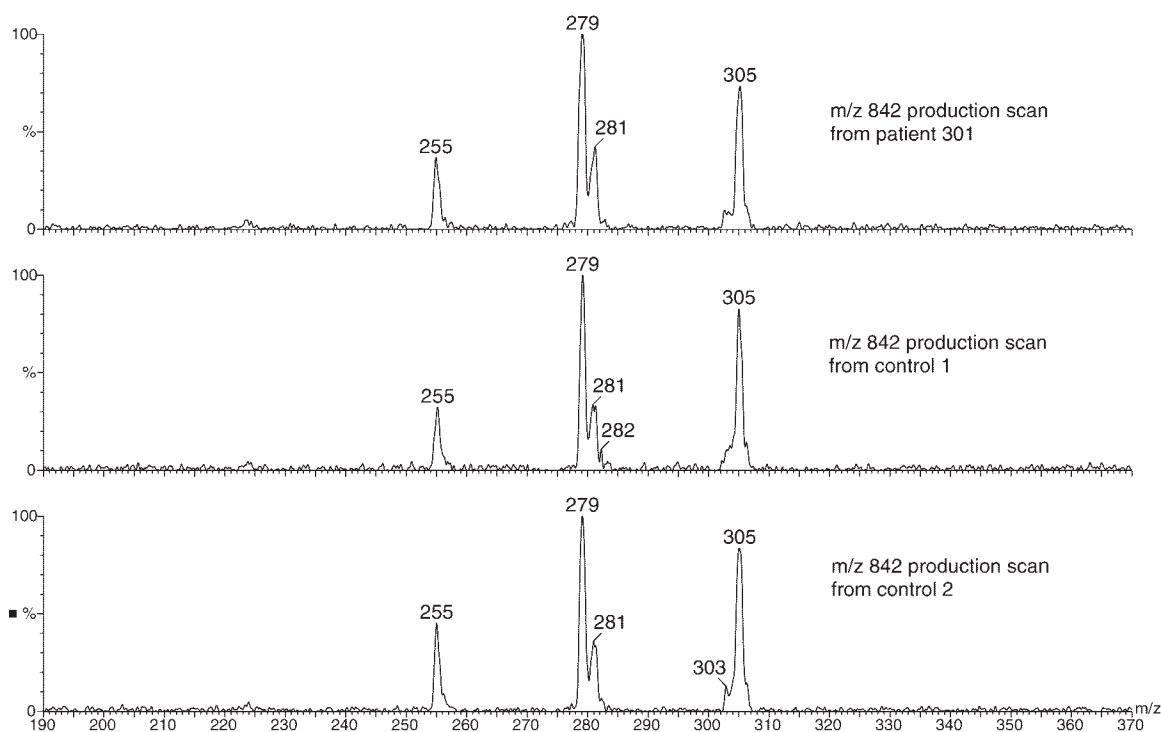


Fig. 4. Comparison of product ions from ESI-MS/MS scans at *m/z* 842 of plasma HDL samples from three different subjects.

and PC species described here and their relative abundances were consistent with what had been reported for other kinds of biological samples, such as blood, red blood cells, and liver homogenates (18, 32–34). We did not acquire product ion spectra for acyl anions of a few minor PCs because their intensities were too low. Although the interpretation of components of diacyl PC species as $[M+CH_3OO]^-$ was definitive in negative ion ESI-MS/MS, we were not able to differentiate between some odd carbon-numbered acyl PCs and ether PCs, in which an alkyl chain is linked to the glycerol backbone via

an ether rather than an ester bond. For instance, both 15:0/18:2 diacyl PC and 18:2/16:0 1-*O*-alkenyl-2-acyl PC produce a pseudomolecular ion at m/z 802 (35). These PCs are listed in the supplementary data and were not taken into account for the PC quantitation. The ether subclass content of PC is known to be relatively low in most tissues, especially in liver, from which HDL particles originate (36, 37). SM and PC species comprising fatty acid moieties with an odd number of carbon atoms are also rare in nature and occur only when the fatty acid synthase uses propionyl-CoA instead of acetyl-CoA in fatty acid biosynthesis

TABLE 4. Characterization and relative quantitation of SM and PC in total HDLs isolated from plasma

m/z^a	Species	Control 1	Control 2	Control 3	Control 4	Subject 303	Subject 301
SM							
675	N14:0	1.87 ± 0.03	2.00 ± 0.05	1.91 ± 0.03	2.17 ± 0.14	4.68 ± 0.24	2.61 ± 0.37
689	N15:0	2.17 ± 0.16	2.08 ± 0.15	1.36 ± 0.01	1.74 ± 0.10	4.13 ± 0.18	2.55 ± 0.31
701	N16:1	4.24 ± 0.16	3.90 ± 0.35	3.82 ± 0.06	5.12 ± 0.25	5.07 ± 0.41	4.69 ± 0.44
703	N16:0	23.66 ± 0.48	25.68 ± 0.71	25.85 ± 0.34	24.82 ± 0.31	52.17 ± 4.92	45.41 ± 3.59
729	N18:1	2.93 ± 0.20	2.35 ± 0.17	2.69 ± 0.20	4.16 ± 0.08	4.03 ± 0.23	3.86 ± 0.49
731	N18:0	3.51 ± 0.27	3.09 ± 0.16	3.94 ± 0.20	4.81 ± 0.15	5.36 ± 0.51	6.24 ± 0.64
759	N20:0	3.71 ± 0.21	4.23 ± 0.97	4.01 ± 0.12	4.52 ± 0.19	4.88 ± 0.90	7.31 ± 0.19
773	N21:0	3.52 ± 0.58	3.61 ± 0.53	3.82 ± 0.54	4.37 ± 0.52	7.66 ± 0.86	4.98 ± 0.93
785	N22:1	7.24 ± 0.75	6.22 ± 0.40	6.89 ± 0.90	10.11 ± 1.43	3.02 ± 1.25	5.21 ± 0.97
787	N22:0	6.22 ± 1.56	5.92 ± 0.25	6.58 ± 1.11	6.57 ± 1.04	4.13 ± 0.51	5.17 ± 2.04
799	N23:1	5.39 ± 1.44	6.11 ± 2.04	3.64 ± 0.51	4.85 ± 0.50	6.63 ± 1.08	4.44 ± 1.03
811	N24:2	10.00 ± 1.47	6.57 ± 1.17	8.41 ± 1.33	9.47 ± 1.03	5.35 ± 0.99	7.40 ± 1.85
813	N24:1	17.25 ± 2.35	13.46 ± 2.06	13.96 ± 1.76	14.74 ± 2.15	12.62 ± 1.52	15.76 ± 2.47
	Sum	91.72 ± 9.09	85.44 ± 7.07	86.88 ± 8.66	97.45 ± 6.30	118.10 ± 9.53	113.19 ± 14.83
PC							
730	C14:0/C18:2	1.47 ± 0.12	0.89 ± 0.13	0.88 ± 0.03	1.34 ± 0.05	3.86 ± 0.38	1.49 ± 0.19
732	C16:0/C16:1 ^b and C14:0/C18:1	6.73 ± 0.53	2.18 ± 0.29	2.65 ± 0.21	3.35 ± 0.26	17.23 ± 0.41	9.69 ± 1.91
734	C16:0/C16:0	3.83 ± 0.18	3.31 ± 0.12	3.36 ± 0.27	2.35 ± 0.26	15.19 ± 0.97	9.15 ± 0.54
756	C16:1/C18:2 ^b and C16:0/C18:3	6.18 ± 0.42	4.02 ± 0.38	4.80 ± 0.28	8.47 ± 0.21	18.53 ± 0.33	9.27 ± 1.38
758	C16:0/C18:2	189.14 ± 7.98	201.52 ± 12.43	208.09 ± 12.89	196.89 ± 13.58	525.50 ± 17.70	285.56 ± 37.97
760	C16:0/C18:1	106.98 ± 6.46	79.28 ± 6.29	64.08 ± 4.69	86.51 ± 5.85	198.93 ± 7.66	173.55 ± 12.66
780	C16:0/C20:5 ^b and C16:1/C20:4 and C18:2/C18:3	14.99 ± 1.04	10.10 ± 0.92	6.95 ± 0.86	11.02 ± 0.47	19.29 ± 2.40	14.85 ± 2.11
782	C16:0/C20:4 ^b and C18:2/C18:2	109.99 ± 6.92	105.41 ± 7.03	61.86 ± 5.24	81.11 ± 5.78	144.80 ± 6.91	142.04 ± 11.45
784	C18:1/C18:2 ^{b,c} and C16:0/C20:3 ^{b,c}	73.70 ± 4.49	69.00 ± 4.51	53.18 ± 4.33	91.96 ± 7.20	182.02 ± 6.90	121.35 ± 21.02
786	C18:0/C18:2 ^b and C18:1/C18:1 and C16:0/C20:2	106.18 ± 5.47	119.02 ± 9.29	117.97 ± 8.84	119.75 ± 9.71	303.39 ± 12.82	224.95 ± 37.43
788	C18:0/C18:1	18.31 ± 1.81	14.87 ± 1.97	11.88 ± 0.90	16.29 ± 0.63	37.56 ± 1.69	37.37 ± 4.35
806	C16:0/C22:6 ^b and C18:2/C20:4 and C18:0/C20:6	57.67 ± 3.87	38.05 ± 2.80	40.21 ± 3.48	50.39 ± 3.37	25.88 ± 1.10	63.99 ± 5.87
808	C16:0/C22:5 ^{b,c} and C18:1/C20:4 ^{b,c} and C18:2/C20:3 and C18:0/C20:5	41.59 ± 2.90	33.18 ± 2.17	19.35 ± 1.97	35.85 ± 2.85	47.72 ± 3.47	55.69 ± 8.83
810	C18:0/C20:4 ^b and C18:1/C20:3 and C16:0/C22:4	64.32 ± 3.79	68.89 ± 4.21	38.48 ± 3.03	50.71 ± 3.74	84.37 ± 4.32	119.30 ± 16.81
812	C18:0/C20:3	21.58 ± 1.53	20.94 ± 1.60	9.76 ± 0.64	20.07 ± 1.43	34.51 ± 2.35	37.53 ± 3.63
832	C18:1/C22:6	5.00 ± 0.51	3.90 ± 0.42	3.29 ± 0.29	5.86 ± 0.14	4.26 ± 0.31	8.09 ± 1.42
834	C18:0/C22:6	19.46 ± 1.59	11.53 ± 0.52	12.30 ± 1.14	14.83 ± 0.39	9.39 ± 0.63	28.84 ± 2.63
836	C18:0/C22:5	7.31 ± 0.69	5.44 ± 0.20	2.99 ± 0.24	4.18 ± 0.27	8.51 ± 0.72	9.12 ± 1.73
	Sum	854.43 ± 47.71	791.55 ± 48.72	662.08 ± 48.98	800.94 ± 54.40	1680.93 ± 63.59	1351.82 ± 145.38
SM/PC ratio		0.11 ± 0.01	0.11 ± 0.01	0.13 ± 0.01	0.12 ± 0.01	0.07 ± 0.01	0.08 ± 0.01

SM, sphingomyelin.

^a Nominal figures.

^b This species is the major one.

^c Both species are equally important.

(38). However, fatty acids with an odd number of carbons (mainly 15 and 17) have been reported, and they apparently correlate with dairy product intake (39).

For quantitative analysis with internal standard addition, we used known amounts of nonnatural phospholipids as internal standards (200.0 nmol C19:0/C19:0 PC and 30.0 nmol N17:0 SM, both of which were shown to be absent in the samples at the beginning of the study), which were co-extracted with the plasma HDL samples. The abundance of PC and SM was then assessed by relating the ratio of the peak height of the plasma analyte to that of the corresponding internal standards. Absolute quantitation (with correction of the chain length and degree of unsaturation

effects on the ion intensities) was performed only for the major SM and PC species (**Table 6**). For all other minor species, we sought only their relative levels in the samples and studied the differences in their magnitudes between control and NPD-B samples in a comparative analysis (Table 4). We demonstrated that plasma HDL from NPD-B was significantly enriched in SM by an average of 28%. The increase was particularly significant if we considered only the major SM species N16:0 SM (67.82 ± 6.40 pmol/mg apoA-I in subject 303 and 59.03 ± 4.67 pmol/mg apoA-I in subject 301 vs. an average of ~ 33 pmol/mg apoA-I in controls, for an increase of 95%). Interestingly, we also observed an increase in total PC levels (95%) compared with

TABLE 5. Characterization and relative quantitation of SM and PC in nascent HDLs generated from fibroblasts

<i>m/z</i> ^a	Species	Control 1	Control 2	Control 3	Control 4	Subject 303	Subject 301
SM							
675	N14:0	0.85 ± 0.10	0.83 ± 0.09	1.25 ± 0.06	1.25 ± 0.10	2.31 ± 0.27	1.67 ± 0.32
689	N15:0	0.78 ± 0.21	0.90 ± 0.23	1.28 ± 0.14	1.75 ± 0.17	2.85 ± 0.73	1.98 ± 0.74
701	N16:1	1.00 ± 0.14	1.09 ± 0.08	1.17 ± 0.02	1.46 ± 0.20	2.20 ± 0.34	1.54 ± 0.25
703	N16:0	6.84 ± 0.40	6.28 ± 0.46	8.98 ± 0.46	6.65 ± 0.50	11.70 ± 0.34	10.24 ± 0.96
715	N17:1	n.d.	n.d.	n.d.	0.50 ± 0.03	0.72 ± 0.12	0.62 ± 0.11
729	N18:1	0.35 ± 0.03	0.46 ± 0.06	0.52 ± 0.07	0.59 ± 0.05	1.02 ± 0.11	1.05 ± 0.41
731	N18:0	0.11 ± 0.03	0.12 ± 0.04	0.27 ± 0.02	0.20 ± 0.09	0.29 ± 0.11	0.29 ± 0.10
773	N21:0	0.46 ± 0.04	0.62 ± 0.06	0.62 ± 0.04	0.84 ± 0.12	1.09 ± 0.14	1.19 ± 0.18
799	N23:1	0.66 ± 0.10	0.82 ± 0.13	0.96 ± 0.18	1.52 ± 0.12	2.06 ± 0.47	1.79 ± 0.32
811	N24:2	0.75 ± 0.12	0.79 ± 0.14	0.99 ± 0.26	0.52 ± 0.31	0.39 ± 0.33	0.63 ± 0.31
813	N24:1	1.23 ± 0.06	1.09 ± 0.18	1.74 ± 0.09	1.04 ± 0.22	1.67 ± 0.03	1.84 ± 0.27
	Sum	13.03 ± 0.76	13.00 ± 0.91	17.78 ± 0.15	16.32 ± 1.63	26.31 ± 1.40	22.84 ± 2.52
PC							
730	C14:0/C18:2	0.57 ± 0.07	0.79 ± 0.05	0.69 ± 0.02	0.93 ± 0.09	0.97 ± 0.17	0.71 ± 0.13
732	C16:0/C16:1 ^b and C14:0/C18:1	5.40 ± 0.76	8.15 ± 0.13	7.57 ± 0.25	7.35 ± 0.62	7.95 ± 0.85	5.71 ± 0.75
734	C16:0/C16:0	30.25 ± 4.14	35.64 ± 1.95	66.03 ± 3.78	36.46 ± 3.63	31.65 ± 2.76	34.14 ± 1.89
756	C16:1/C18:2 ^b and C16:0/C18:3	0.54 ± 0.07	0.76 ± 0.06	0.69 ± 0.10	0.99 ± 0.14	0.93 ± 0.20	0.80 ± 0.09
758	C16:0/C18:2 ^b and C16:1/C18:1	6.74 ± 0.91	9.73 ± 0.23	8.32 ± 0.25	10.65 ± 0.99	9.78 ± 1.23	8.10 ± 1.01
760	C16:0/C18:1	18.91 ± 2.48	27.07 ± 1.08	26.38 ± 0.91	25.55 ± 3.13	23.48 ± 2.17	18.99 ± 2.21
778	C16:0/C20:5 ^b and C16:1/C20:4 and C18:2/C18:3	1.37 ± 0.16	1.69 ± 0.06	1.87 ± 0.85	3.78 ± 0.72	1.93 ± 0.20	1.93 ± 0.59
782	C16:0/C20:4 ^b and C18:2/C18:2	3.10 ± 0.39	4.44 ± 0.18	3.89 ± 0.31	5.79 ± 0.69	4.46 ± 0.63	3.15 ± 0.43
784	C18:1/C18:2 ^{b,c} and C16:0/C20:3 ^{b,c}	2.39 ± 0.28	3.20 ± 0.18	2.69 ± 0.08	4.52 ± 0.30	3.85 ± 0.52	3.16 ± 0.32
786	C18:0/C18:2 ^{b,c} and C18:1/C18:1 ^{b,c}	6.98 ± 0.95	10.04 ± 0.05	8.55 ± 0.27	11.12 ± 1.09	10.22 ± 1.14	8.52 ± 1.22
788	C18:0/C18:1	6.06 ± 0.78	9.02 ± 0.38	7.45 ± 0.30	8.92 ± 1.07	8.10 ± 1.00	6.11 ± 0.67
806	C16:0/C22:6 ^b and C18:2/C20:4 and C18:0/C20:6	0.42 ± 0.05	0.64 ± 0.04	0.51 ± 0.10	0.89 ± 0.10	0.67 ± 0.13	0.57 ± 0.07
808	C16:0/C22:5 ^{b,c} and C18:1/C20:4 ^{b,c} and C18:2/C20:3 and C18:0/C20:5	1.15 ± 0.09	1.70 ± 0.04	1.49 ± 0.13	2.15 ± 0.13	2.06 ± 0.26	1.48 ± 0.24
810	C18:0/C20:4 ^b and C18:1/C20:3 and C16:0/C22:4	4.10 ± 0.39	5.26 ± 0.05	5.54 ± 0.19	7.77 ± 0.91	6.08 ± 0.61	4.40 ± 0.62
812	C18:0/C20:3	1.22 ± 0.14	1.22 ± 0.12	1.24 ± 0.10	2.03 ± 0.27	1.57 ± 0.23	1.15 ± 0.16
832	C18:1/C22:6	0.48 ± 0.13	0.64 ± 0.09	0.57 ± 0.06	1.37 ± 0.09	0.52 ± 0.09	0.52 ± 0.05
834	C18:0/C22:6	0.35 ± 0.04	0.55 ± 0.05	0.47 ± 0.15	0.72 ± 0.07	0.63 ± 0.15	0.58 ± 0.09
836	C18:0/C22:5	0.56 ± 0.04	0.81 ± 0.05	0.75 ± 0.09	0.94 ± 0.05	0.85 ± 0.18	0.71 ± 0.10
	Sum	90.61 ± 11.45	121.35 ± 2.66	144.70 ± 5.71	131.94 ± 13.74	115.71 ± 12.16	100.73 ± 8.87
SM/PC ratio		0.15 ± 0.02	0.11 ± 0.01	0.13 ± 0.01	0.12 ± 0.02	0.23 ± 0.02	0.23 ± 0.01

n.d., not detectable.

^a Nominal figures.

^b This species is the major one.

^c Both species are equally important.

TABLE 6. Absolute quantitation of major SM and PC constituents in total HDLs isolated from plasma

Species	Control 1	Control 2	Control 3	Control 4	Subject 303	Subject 301
SM (pmol/mg apoA-I)						
N16:0	30.76 ± 0.62	33.38 ± 0.92	33.61 ± 0.44	32.27 ± 0.40	67.82 ± 6.40 ^a	59.03 ± 4.67 ^b
PC (pmol/mg apoA-I)						
C16:0/C18:2	122.74 ± 5.18	130.77 ± 8.07	135.04 ± 8.36	127.77 ± 8.81	341.01 ± 11.49	185.31 ± 24.64
C16:0/C18:1	74.61 ± 4.51	55.29 ± 4.39	44.69 ± 3.27	60.34 ± 4.08	138.74 ± 5.34	121.04 ± 8.83
C16:0/C20:4 and C18:2/C18:2	72.31 ± 4.55	69.30 ± 4.62	40.67 ± 3.45	53.33 ± 3.80	95.20 ± 4.54	93.39 ± 7.53
C18:1/C18:2 and C16:0/C20:3	51.63 ± 3.15	48.34 ± 3.16	37.26 ± 3.03	64.42 ± 5.04	127.52 ± 4.83	85.03 ± 14.75
C18:0/C18:2 and C18:1/C18:1 and C16:0/C20:2	78.91 ± 4.07	88.46 ± 6.90	87.68 ± 6.57	89.00 ± 7.22	225.48 ± 9.53	167.19 ± 27.82
Sum	400.20 ± 21.46	392.16 ± 27.14	345.34 ± 24.68	394.86 ± 28.95	928.95 ± 35.73 ^c	651.96 ± 83.57 ^d

apoA-I, apolipoprotein A-I. The absolute quantities of SM and PC were calculated from the ion intensities obtained in electrospray ionization-mass spectrometry corrected with the chain length and degree of saturation effects estimated in Table 3 as described in Materials and Methods. Each value represents the mean ± SD of three preparations.

^a $P < 0.01$ compared with the average of control samples.

^b $P < 0.01$ compared with the average of control samples.

^c $P < 0.001$ compared with the average of control samples.

^d $P = 0.015$ compared with the average of control samples.

that of palmitoyl SM in plasma HDL extracted from NPD-B with respect to normal subjects. This increase was spread evenly across all of the PC species present. The sum of the nine dominant PC species was calculated as 928.95 ± 35.73 pmol/mg apoA-I in subject 303 and 651.96 ± 83.57 pmol/mg apoA-I in subject 301 versus an average of ~ 383 pmol/mg apoA-I in controls. Accordingly, the SM-to-PC ratio in plasma HDL samples from diseased subjects was not increased but slightly decreased (SM/PC ranging from 0.07 to 0.13). The nearly constant SM-to-PC ratios were also observed when using the HPLC/MS system on the same samples (data not shown). The values obtained here were within the biological range reported in various studies using mass spectrometry (33, 34).

Increased levels of SM in nascent HDLs generated from NPD-B fibroblasts

Similar to the plasma HDL samples, HDL samples nascently generated in tissue culture were subjected to qualitative and quantitative analysis, using 4.0 nmol of PC C19:0/C19:0 and 1.5 nmol of SM N17:0 internal standards (Table 5, Table 7, Fig. 8). There was a considerable difference in terms of the quantity of lipids between the total HDLs purified from plasma and the nascent HDLs generated from

fibroblast cells: the SM and PC content was more than 10-fold higher in the plasma HDL fractions than in the nascent HDLs. In addition, even though similar SM and PC species were identified, their relative abundances were significantly different. For instance, in HDL samples generated in vitro, SM with shorter chain length (SM N14:0) became as prevalent as SM N24:1 and N24:2. Also, di-palmitoyl (16:0/16:0) PC became the most abundant PC species (27–46% of total PC content), followed by oleoyl-palmitoyl (18:1/16:0) PC, linoleoyl-stearoyl (18:2/18:0) PC, di-oleoyl (18:1/18:1) PC, linoleoyl-palmitoyl (18:2/16:0) PC, oleoyl-palmitoleoyl (18:1/16:1) PC, and oleoyl-stearoyl (18:1/18:0) PC. However, we observed an equivalent increase in total SM level (average of $\sim 63\%$) when the HDL was generated from NPD-B fibroblasts. The major SM constituent, SM N16:0, was calculated to be 11.93 ± 0.35 pmol/mg apoA-I/mg cell protein in subject 303 and 10.44 ± 0.98 pmol/mg apoA-I/mg cell protein in subject 301 versus an average of ~ 7.3 pmol/mg apoA-I/mg cell protein in controls. Interestingly, although there was a concomitant increase in total PC level in plasma HDL extracted from NPD-B subjects, the PC level in nascent HDLs generated from NPD-B cells was comparable to that of controls (ranging from ~ 50 – 85 pmol/mg apoA-I/mg cell protein; the average of the two patients had a two-tail $P > 0.10$).

TABLE 7. Absolute quantitation of SM and PC constituents in nascent HDLs generated from fibroblasts

Species	Control 1	Control 2	Control 3	Control 4	Subject 303	Subject 301
SM (pmol/mg apoA-I/mg cell proteins)						
N16:0	6.98 ± 0.41	6.41 ± 0.47	9.16 ± 0.47	6.78 ± 0.51	11.93 ± 0.35 ^a	10.44 ± 0.98 ^b
PC (pmol/mg apoA-I/mg cell proteins)						
C16:0/C16:0	21.45 ± 2.94	25.28 ± 1.38	46.83 ± 2.68	25.86 ± 2.57	22.45 ± 1.96	24.21 ± 1.34
C16:0/C18:2 and C16:1/C18:1	4.96 ± 0.67	7.16 ± 0.17	6.12 ± 0.18	7.84 ± 0.73	7.20 ± 0.91	5.96 ± 0.74
C16:0/C18:1	14.32 ± 1.88	20.05 ± 0.82	19.97 ± 0.69	19.34 ± 2.37	17.78 ± 1.64	14.38 ± 1.67
C18:0/C18:2 and C18:1/C18:1	5.72 ± 0.78	8.23 ± 0.04	7.01 ± 0.22	9.12 ± 0.89	8.38 ± 0.93	6.98 ± 1.00
C18:0/C18:1	5.11 ± 0.66	7.61 ± 0.32	6.28 ± 0.25	7.52 ± 0.90	6.83 ± 0.84	5.15 ± 0.57
Sum	51.56 ± 6.93	68.33 ± 2.73	86.21 ± 4.02	69.68 ± 7.46	62.64 ± 6.28 ^c	56.68 ± 5.32 ^d

The absolute quantities of SM and PC were calculated from the ion intensities corrected with the chain length and degree of saturation effects estimated in Table 3 as described in Materials and Methods. Each value represents the mean ± SD of three preparations.

^a $P < 0.001$ compared with the average of control samples.

^b $P < 0.01$ compared with the average of control samples.

^c $P > 0.01$ compared with the average of control samples.

^d $P < 0.001$ compared with the average of control samples.

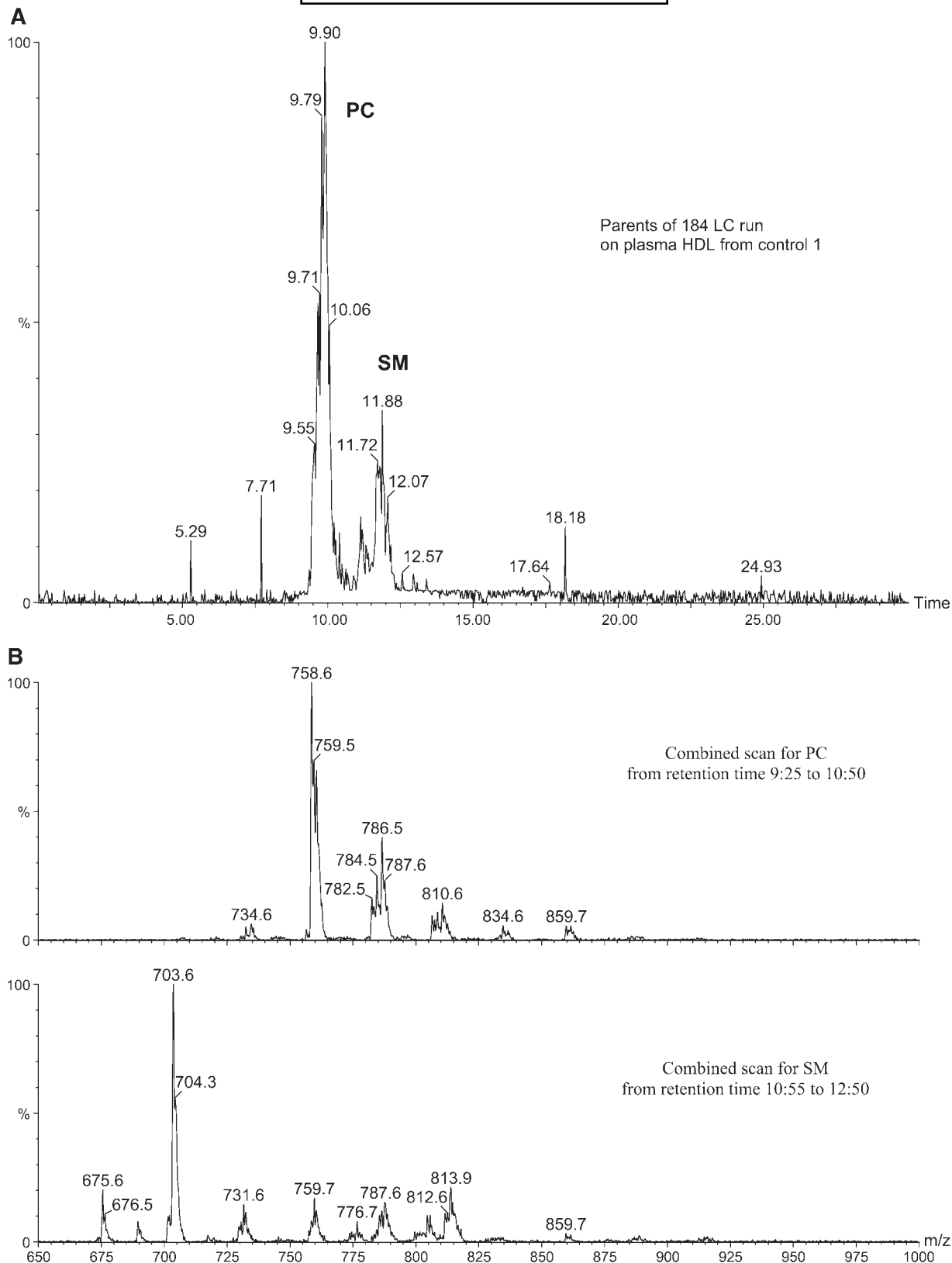


Fig. 5. SM and PC analyses by HPLC-MS. A: HPLC run of plasma HDL from control 1 using the parent ion mode at m/z 184. Only the PC and SM species appeared in the spectrum, as a result of their common phosphocholine head group. B: Major PC and SM species eluted from retention times 9:25 to 10:50 and 10:55 to 12:50, respectively.

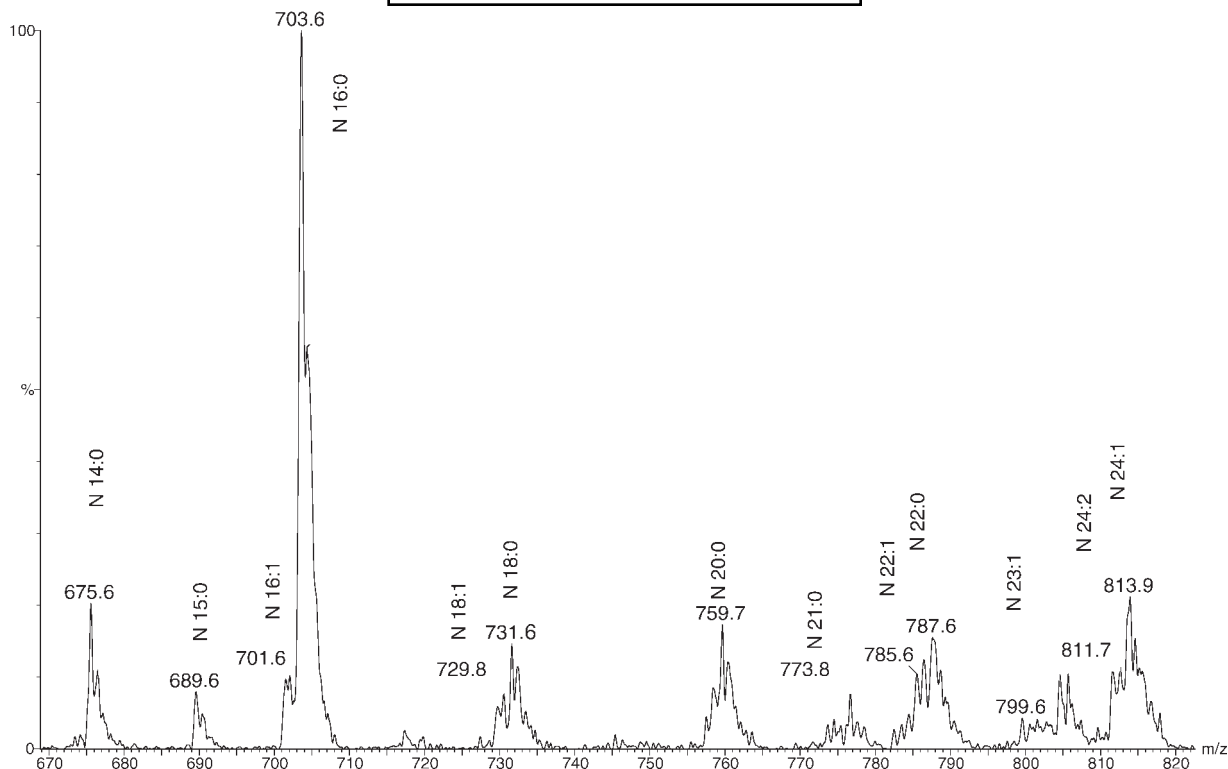


Fig. 6. An expansion of Figure 5B from m/z 665 to m/z 825 where SM species were annotated.

Therefore, these patients' HDLs have a significant increase in SM-to-PC ratio (0.23 vs. an average of 0.13 in controls, for an 80% increase). Furthermore, this SM-to-PC ratio was more than 2.5-fold higher in nascent HDLs generated by our system than in the total plasma HDLs. We note that the total HDL fraction from human plasma was heterogeneous and was composed of different types of HDL particles, whose lipid composition is dependent on the stage in their maturation process (40). Overall, our quantitation method has been validated by calibration curves prepared by mixing N17:0 SM and C19:0/C19:0 PC standards in working ranges with varying amounts of analyte. The calibration curves were constructed by determining the ratio of the peak heights of the analytes to that of the corresponding internal standards (data not shown). Also, by comparison of two sets of triplicate experiments using the addition of the standard either before or after extraction, we determined that our extraction method had a relatively high yield (greater than 85%) and that the variations between each extraction were less than 3% (data not shown).

DISCUSSION

Mass spectrometry is a very powerful tool for analyzing intact phospholipid molecular species without the need for derivatization, with decreased risk of artifacts and increased reproducibility and sensitivity. Because of the positively charged quaternary ammonium of the choline head group, PC and SM were readily detected in positive ion mode with femtomole to picomole sensitivity. CID of cat-

ions of both SM and PC yielded a characteristic fragment of the phosphorylcholine moiety at m/z 184, enabling their profiling in unprocessed lipid extracts by precursor ion scanning. Also, PC and SM were readily discriminated by the nitrogen rule (41), because monoprotonated molecular ions of PC have even nominal masses, whereas ions of SM exhibit odd nominal masses. This is attributable to the presence of an additional nitrogen in SM. Our SM and PC species characterization was supported by a collaborative study performed separately by ESI-MS coupled online with HPLC, which allowed chromatographic separation of SM and PC before MS analysis and prevented the confusion caused by ions hidden in the overlapping peak clusters.

With ESI-MS/MS, we were able to measure qualitatively and quantitatively for the first time the SM and PC profiles of HDL particles, which is usually expressed as total mole percentage of total lipids only (42). The reason for this probably is that lipid characterization and quantitation in these complex samples have been relatively complicated and time-consuming. Despite the ability to characterize the acyl chains of each species in this study, the *sn* positions of the individual acyl residues and the double bond positions were not determined by our current method (43). The relative quantitation of the SM and PC analytes was performed by internal standard addition using a known quantity of the nonnatural standards N17:0 SM and C19:0/C19:0 PC. The true molar abundances of the major SM and PC species were then estimated by correcting the effects of chain length and degree of unsaturation. Although attention has been paid to the effects of concentration on ion intensities (calibration curves were constructed with

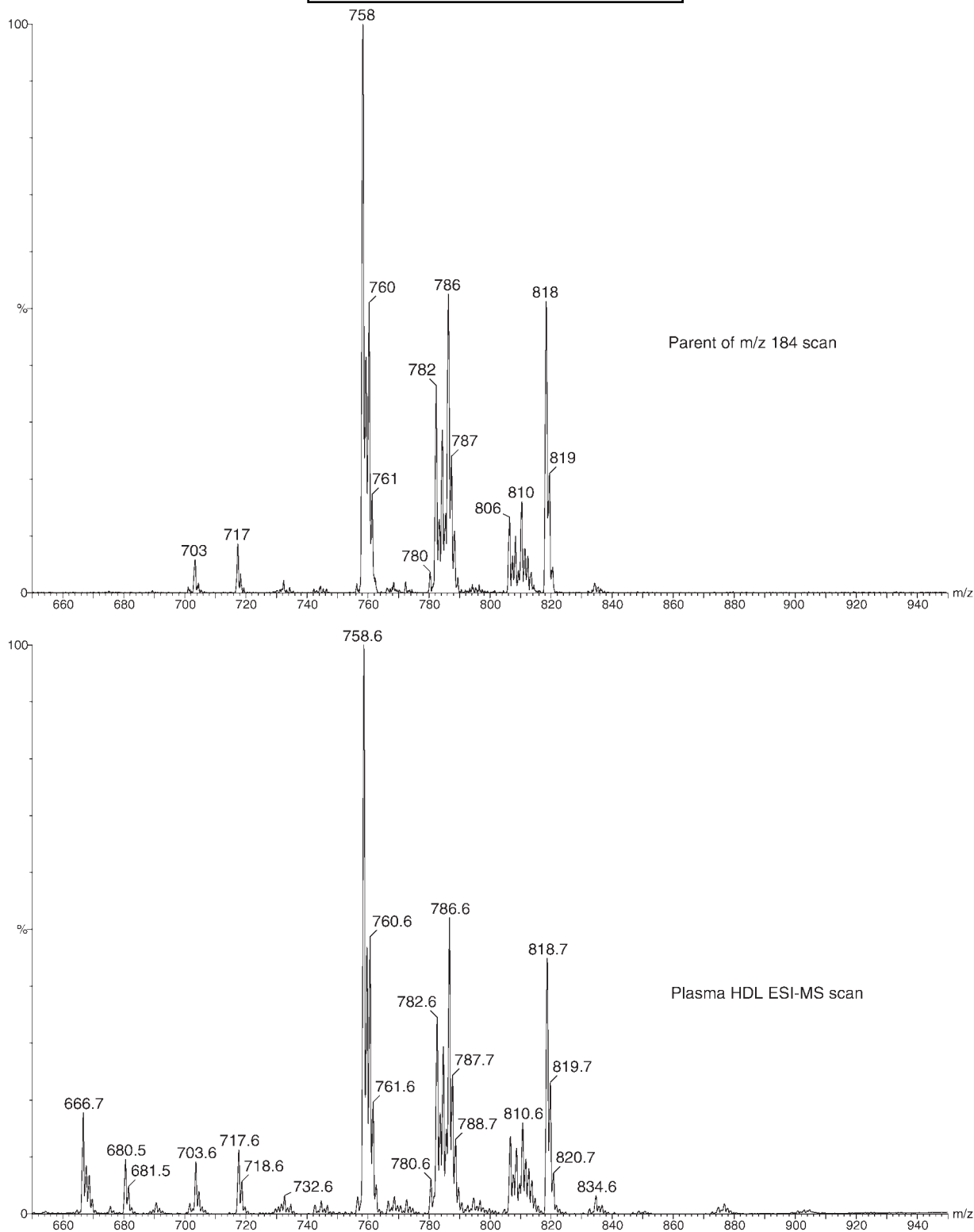


Fig. 7. ESI-MS scan of HDL isolated from plasma and its corresponding parent ion spectrum at m/z 184 (scan range of 650–950 Da) in the positive ion mode. Extracted lipids were diluted 42-fold in chloroform-methanol (1:2) containing 25 mM ammonium acetate. The m/z 717 and 818 peaks represent N17:0 SM and C19:0 PC (30.0 and 200.0 nmol in 200 μ l of chloroform, respectively) standards added to the HDL samples before lipid extraction.

standards of two different concentrations, 200.0 and 4.0 nmol of PC), it should be noted that our calculation was done with the assumption that the effects of concentration within each sample (at least for the major SM and PC species with

respect to the N17:0 SM and C19:0/C19:0 PC standards) were negligible. We found that the SM content in HDLs from NPD-B was higher than normal by at least 28%, which could be attributed to their deficiency of SMase activity.

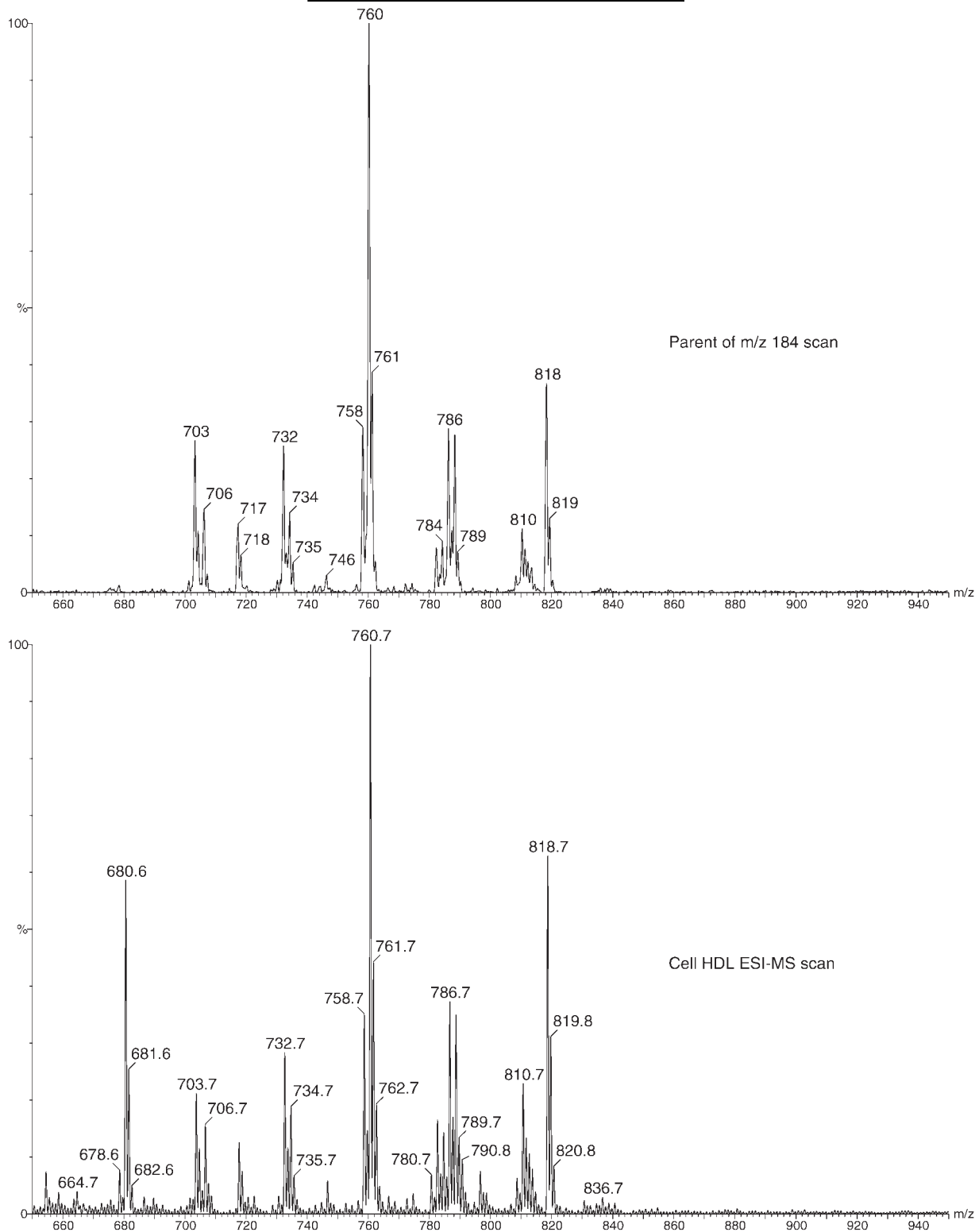



Fig. 8. ESI-MS scan of HDL generated from fibroblasts and its corresponding parent ion spectrum at m/z 184. The experimental conditions of ESI-MS analysis were the same as those for plasma HDL samples. Extracted lipids were diluted 14-fold in chloroform-methanol (1:2) containing 25 mM ammonium acetate. The m/z 717 and 818 peaks represent N17:0 SM and C19:0 PC (1.5 and 4.0 nmol in 200 μ l of chloroform, respectively) standards added to the HDL samples before lipid extraction.

The finding that the HDLs extracted from plasma and generated in vitro from tissue culture of NPD-B subjects was enriched in SM compared with controls is significant because of the condensing capacity of SM. It has been pro-

posed that the presence of SM modulates amphiphilic peptide and protein interaction with the membrane interface (44). Therefore, its level in lipoproteins could highly affect their conformation and functions. MS could be useful

in the diagnosis of NPD-B as well as other lipid abnormalities. Most importantly, the comprehensive characterization and quantitation of lipid in HDLs by MS will be important for the better understanding of arteriosclerosis (45) and will have significant impact on lipid research. 

This research was supported by the Canadian Institute of Health Research (Grants MOP 15042, MOP 62834, and MT-6712). The authors express their thanks to Shiona Dempster for excellent technical assistance.

REFERENCES

- Spence, M. W., and J. W. Callahan. 1989. Sphingomyelin-cholesterol lipidoses: the Niemann-Pick group of diseases. *In* The Metabolic Basis of Inherited Disease II. J. B. Stanbury, J. B. Wyngaarden, and D. S. Frederickson, editors. McGraw-Hill, New York. 1655–1676.
- Kudoh, T., M. A. Velkoff, and D. A. Wenger. 1983. Uptake and metabolism of radioactively labeled sphingomyelin in cultured skin fibroblasts from controls and patients with Niemann-Pick disease and other lysosomal storage diseases. *Biochim. Biophys. Acta.* **754**: 82–92.
- Lee, C. Y., L. Krimbou, J. Vincent, C. Bernard, P. Larramee, J. Genest, Jr., and M. Marcil. 2003. Compound heterozygosity at the sphingomyelin phosphodiesterase-1 (SMPD1) gene is associated with low HDL cholesterol. *Hum. Genet.* **112**: 52–62.
- Genest, J. 2003. Lipoprotein disorders and cardiovascular risk. *J. Inherit. Metab. Dis.* **26**: 267–287.
- Fielding, C. J., and P. E. Fielding. 1995. Molecular physiology of reverse cholesterol transport. *J. Lipid Res.* **36**: 211–228.
- Sparks, D. L., P. G. Frank, S. Braschi, T. A. Neville, and Y. L. Marcel. 1999. Effect of apolipoprotein A-I lipidation on the formation and function of pre- β and α -migrating LpA-I particles. *Biochemistry.* **38**: 1727–1735.
- Sparks, D. L., W. S. Davidson, S. Lund-Katz, and M. C. Phillips. 1995. Effects of the neutral lipid content of high density lipoprotein on apolipoprotein A-I structure and particle stability. *J. Biol. Chem.* **270**: 26910–26917.
- Philips, G. B., and J. T. Doges. 1967. Composition of phospholipids and phospholipid fatty acids of human plasma. *J. Lipid Res.* **8**: 676–681.
- Helms, J. B., and C. Zurzolo. 2004. Lipids as targeting signals: lipid rafts and intracellular trafficking. *Traffic.* **5**: 247–254.
- Ahmed, S. N., D. A. Brown, and E. London. 1997. On the origin of sphingolipid/cholesterol-rich detergent-insoluble cell membranes: physiological concentrations of cholesterol and sphingolipid induce formation of a detergent-insoluble, liquid-ordered lipid phase in model membranes. *Biochemistry.* **36**: 10944–10953.
- Bolin, D. J., and A. Jonas. 1996. Sphingomyelin inhibits the lecithin-cholesterol acyltransferase reaction with reconstituted high density lipoproteins by decreasing enzyme binding. *J. Biol. Chem.* **271**: 19152–19158.
- Rye, K. A., N. J. Hime, and P. J. Barter. 1996. The influence of sphingomyelin on the structure and function of reconstituted high density lipoproteins. *J. Biol. Chem.* **271**: 4243–4250.
- Bernstrom, K., K. Kayganich, and R. C. Murphy. 1991. Collisionally induced dissociation of epoxyeicosatrienoic acids and epoxyeicosatrienoic acid-phospholipid molecular species. *Anal. Biochem.* **198**: 203–211.
- Han, X., and R. W. Gross. 1994. Electrospray ionization mass spectroscopic analysis of human erythrocyte plasma membrane phospholipids. *Proc. Natl. Acad. Sci. USA.* **91**: 10635–10639.
- Kerwin, J. L., A. R. Tuininga, and L. H. Ericsson. 1994. Identification of molecular species of glycerophospholipids and sphingomyelin using electrospray mass spectrometry. *J. Lipid Res.* **35**: 1102–1114.
- Marcil, M., B. Boucher, L. Krimbou, B. C. Solymoss, J. Davignon, J. Frohlich, and J. Genest, Jr. 1995. Severe familial HDL deficiency in French-Canadian kindreds. Clinical, biochemical, and molecular characterization. *Arterioscler. Thromb. Vasc. Biol.* **15**: 1015–1024.
- Poumay, Y., and M. F. Ronveaux-Dupal. 1985. Rapid preparative iso-

- lation of concentrated low density lipoprotein and lipoprotein-deficient serum using vertical rotor gradient ultracentrifugation. *J. Lipid Res.* **26**: 1476–1480.
- Uran, S., A. Larsen, P. B. Jacobsen, and T. Skotland. 2001. Analysis of phospholipid species in human blood using normal-phase liquid chromatography coupled with electrospray ionization ion-trap tandem mass spectrometry. *J. Chromatogr. B Biomed. Sci. Appl.* **758**: 265–275.
- Koc, H., M. H. Mar, A. Ranasinghe, J. A. Swenberg, and S. H. Zeisel. 2002. Quantitation of choline and its metabolites in tissues and foods by liquid chromatography/electrospray ionization-isotope dilution mass spectrometry. *Anal. Chem.* **74**: 4734–4740.
- Han, X., and R. W. Gross. 2003. Global analyses of cellular lipidomes directly from crude extracts of biological samples by ESI mass spectrometry: a bridge to lipidomics. *J. Lipid Res.* **44**: 1071–1079.
- Koivusalo, M., P. Haimi, L. Heikinheimo, R. Kostianen, and P. Somerharju. 2001. Quantitative determination of phospholipid compositions by ESI-MS: effects of acyl chain length, unsaturation, and lipid concentration on instrument response. *J. Lipid Res.* **42**: 663–672.
- Brugger, B., G. Erben, R. Sandhoff, F. T. Wieland, and W. D. Lehmann. 1999. Quantitative analysis of biological membrane lipids at the low picomole level by nano-electrospray ionization tandem mass spectrometry. *Proc. Natl. Acad. Sci. USA.* **94**: 2339–2344.
- DeLong, C. J., P. R. Baker, M. Samuel, Z. Cui, and M. J. Thomas. 2001. Molecular species composition of rat liver phospholipids by ESI-MS/MS: the effect of chromatography. *J. Lipid Res.* **42**: 1959–1968.
- Lin, Z., A. Mateo, Y. Zheng, E. Kesselman, E. Pancallo, D. J. Hart, Y. Talmon, H. T. Davis, L. E. Scriven, and J. L. Zakin. 2002. Comparison of drag reduction, rheology, microstructure and stress-induced precipitation of dilute cationic surfactant solutions with odd and even alkyl chains. *Rheol. Acta.* **41**: 483–492.
- Toshimi, S. 2000. New aspects of surfactants: formation of high axial-ratio microstructures from sugar-, peptides-, and nucleobase-based bolaamphiphiles. *Nihon Yukagakkaishi.* **49**: 1261–1270.
- Pulfer, M., and R. C. Murphy. 2003. Electrospray mass spectrometry of phospholipids. *Mass Spectrom. Rev.* **22**: 332–364.
- Houjou, T., K. Yamatani, H. Nakanishi, M. Imagawa, T. Shimizu, and R. Taguchi. 2004. Rapid and selective identification of molecular species in phosphatidylcholine and sphingomyelin by conditional neutral loss scanning and MS³. *Rapid Commun. Mass Spectrom.* **18**: 3123–3130.
- Hsu, F. F., and J. Turk. 2003. Electrospray ionization/tandem quadrupole mass spectrometric studies on phosphatidylcholines: the fragmentation processes. *J. Am. Soc. Mass Spectrom.* **14**: 352–363.
- Cheng, C., and M. L. Gross. 2000. Applications and mechanisms of charge-remote fragmentation. *Mass Spectrom. Rev.* **19**: 398–420.
- Hsu, F. F., and J. Turk. 1999. Structural determination of sphingomyelin by tandem mass spectrometry with electrospray ionization. *J. Am. Soc. Mass Spectrom.* **11**: 437–449.
- Unknown authors. 1975. Blood-lipids. *In* Scientific Tables-Documenta Geigy. 7th edition. K. Diem and C. Lentner, editors. Thieme Verlag, Stuttgart, Germany. 601–604.
- Malavolta, M., F. Bocci, E. Boselli, and N. G. Frega. 2004. Normal phase liquid chromatography-electrospray ionization tandem mass spectrometry analysis of phospholipid molecular species in blood mononuclear cells: application to cystic fibrosis. *J. Chromatogr. B Anal. Technol. Biomed. Life Sci.* **810**: 73–86.
- Tserng, K. Y., and R. Griffin. 2003. Quantitation and molecular species determination of diacylglycerols, phosphatidylcholines, ceramides, and sphingomyelins with gas chromatography. *Anal. Biochem.* **323**: 84–93.
- Pike, L. J., X. Han, K. N. Chung, and R. W. Gross. 2002. Lipid rafts are enriched in arachidonic acid and plasmenylethanolamine and their composition is independent of caveolin-1 expression: a quantitative electrospray ionization/mass spectrometric analysis. *Biochemistry.* **41**: 2075–2088.
- Liebisch, G., B. Lieser, J. Rathenber, W. Drobnik, and G. Schmitz. 2004. High-throughput quantitation of phosphatidylcholine and sphingomyelin by electrospray ionization tandem mass spectrometry coupled with isotope correction algorithm. *Biochim. Biophys. Acta.* **1686**: 108–117.
- Paltauf, F. 1994. Ether lipids in biomembranes. *Chem. Phys. Lipids.* **74**: 101–139.
- Guan, Z., J. Grunler, S. Piao, and P. J. Sindelar. 2001. Separation and quantitation of phospholipids and their ether analogues by high-performance liquid chromatography. *Anal. Biochem.* **297**: 137–143.

38. Michal G. 1999. *Biochemical Pathways: An Atlas of Biochemistry and Molecular Biology*. John Wiley & Sons, New York. 76.
39. Baylin, A., E. K. Kabagambe, X. Siles, and H. Campos. 2002. Adipose tissue biomarkers of fatty acid intake. *Am. J. Clin. Nutr.* **76**: 750–757.
40. Leroy, A., J. Dallongeville, and J. Fruchart. 1995. Apolipoprotein A-I-containing lipoproteins and atherosclerosis. *Curr. Opin. Lipidol.* **6**: 281–285.
41. McLafferty, F. W., and F. Turecek. 1993. The nitrogen rule. In *Interpretation of Mass Spectra*. 4th edition. A. Kelly, editor. University Science Books, Mill Valley, CA. 37–38.
42. Perova, N. V., I. N. Ozerova, I. V. Paramonova, A. M. Olfer'ev, N. M. Akhmedzhanov, L. I. Pavlova, and R. G. Oganov. 2001. Phospholipid composition of high-density lipoproteins reflects lipolysis of triglyceride-rich lipoproteins during hyperlipidemia. *Bull. Exp. Biol. Med.* **131**: 321–324.
43. Ekroos, K., C. S. Ejsing, U. Bahr, M. Karas, K. Simons, and A. Shevchenko. 2003. Charting molecular composition of phosphatidylcholines by fatty acid scanning and ion trap MS3 fragmentation. *J. Lipid Res.* **44**: 2181–2192.
44. Steinbauer, B., T. Mehnert, and K. Beyer. 2003. Hydration and lateral organization in phospholipid bilayers containing sphingomyelin: a ^2H -NMR study. *Biophys. J.* **85**: 1013–1024.
45. Asztalos, B. F., for the HDL Atherosclerosis Treatment Study. 2004. High-density lipoprotein metabolism and progression of atherosclerosis: new insights from the HDL Atherosclerosis Treatment Study. *Curr. Opin. Cardiol.* **19**: 385–391.